





Article

PKC β Facilitates Leukemogenesis in Chronic Lymphocytic Leukaemia by Promoting Constitutive BCR-Mediated Signalling

Jodie Hay ^{1,2,†} , Anuradha Tarafdar ^{1,†}, Ailsa K. Holroyd ¹, Hothri A. Moka ¹, Karen M. Dunn ^{1,2} , Alzahra Alshayeb ³, Bryony H. Lloyd ³, Jennifer Cassels ^{1,2}, Natasha Malik ¹, Ashfia F. Khan ¹, IengFong Sou ¹, Jamie Lees ^{1,2}, Hassan N. B. Almuhanha ^{1,2}, Nagesh Kalakonda ³, Joseph R. Slupsky ³  and Alison M. Michie ^{1,2,*} 

¹ School of Cancer Sciences, College of Medicine, Veterinary and Life Sciences, University of Glasgow, Glasgow G12 8QQ, UK

² Paul O’Gorman Leukaemia Research Centre, Gartnavel General Hospital, 21 Shelley Road, Glasgow G12 0ZD, UK

³ Institute of Systems, Molecular and Integrative Biology, University of Liverpool, Liverpool L69 7BE, UK

* Correspondence: alison.michie@glasgow.ac.uk; Tel.: +44-(0)141-301-7885

† These authors contributed equally to this work.

Simple Summary: Chronic lymphocytic leukaemia (CLL) is the most common blood cancer in the Western world and remains incurable. While a cause for this cancer has not been defined, one specific protein, protein kinase C β II (PKC β II), is highly expressed in CLL cells and is linked with a poorer clinical outcome. This study shows that PKC β expression plays a central role in assisting the development of leukemic cells in our CLL mouse model. Moreover, a ubiquitously expressed protein SP1 is important for driving the genetic program that promotes leukaemia in our model system, and this program is assisted by PKC β . Importantly, this SP1-driven program is also observed in human CLL cells, suggesting a role for PKC β in the development of human disease.



Citation: Hay, J.; Tarafdar, A.; Holroyd, A.K.; Moka, H.A.; Dunn, K.M.; Alshayeb, A.; Lloyd, B.H.; Cassels, J.; Malik, N.; Khan, A.F.; et al. PKC β Facilitates Leukemogenesis in Chronic Lymphocytic Leukaemia by Promoting Constitutive BCR-Mediated Signalling. *Cancers* **2022**, *14*, 6006. <https://doi.org/10.3390/cancers14236006>

Academic Editor: H. Denis Alexander

Received: 6 October 2022

Accepted: 30 November 2022

Published: 6 December 2022

Publisher’s Note: MDPI stays neutral with regard to jurisdictional claims in published maps and institutional affiliations.



Copyright: © 2022 by the authors. Licensee MDPI, Basel, Switzerland. This article is an open access article distributed under the terms and conditions of the Creative Commons Attribution (CC BY) license (<https://creativecommons.org/licenses/by/4.0/>).

Abstract: B cell antigen receptor (BCR) signalling competence is critical for the pathogenesis of chronic lymphocytic leukaemia (CLL). Defining key proteins that facilitate these networks aid in the identification of targets for therapeutic exploitation. We previously demonstrated that reduced PKC α function in mouse hematopoietic stem/progenitor cells (HPSCs) resulted in PKC β II upregulation and generation of a poor-prognostic CLL-like disease. Here, *prkcb* knockdown in HSPCs leads to reduced survival of PKC α -KR-expressing CLL-like cells, concurrent with reduced expression of the leukemic markers CD5 and CD23. SP1 promotes elevated expression of *prkcb* in PKC α -KR expressing cells enabling leukemogenesis. Global gene analysis revealed an upregulation of genes associated with B cell activation in PKC α -KR expressing cells, coincident with upregulation of PKC β II: supported by activation of key signalling hubs proximal to the BCR and elevated proliferation. Ibrutinib (BTK inhibitor) or enzastaurin (PKC β II inhibitor) treatment of PKC α -KR expressing cells and primary CLL cells showed similar patterns of Akt/mTOR pathway inhibition, supporting the role for PKC β II in maintaining proliferative signals in our CLL mouse model. Ibrutinib or enzastaurin treatment also reduced PKC α -KR-CLL cell migration towards CXCL12. Overall, we demonstrate that PKC β expression facilitates leukemogenesis and identify that BCR-mediated signalling is a key driver of CLL development in the PKC α -KR model.

Keywords: CLL; PKC β ; SP1; BCR signalling; leukemogenesis

1. Introduction

Intracellular signals transmitted through the B cell antigen receptor (BCR) regulate B cell differentiation, survival and proliferation at distinct stages of development, maturation and activation, and play a critical role in driving the pathogenesis of chronic lymphocytic leukaemia (CLL) [1]. The BCR is a critical prognostic marker of CLL, with sequences

aligning closely with germline (>98% similarity; unmutated IgHV) generally associated with poor prognostic CLL cases [2]. The structure of the BCR appears to be related to its ability to transmit and activate intracellular signalling networks more efficiently, thus promoting CLL cell survival and proliferation [3]. BCR crosslinking promotes membrane localisation and activation of a number of cytoplasmic protein kinases including Lyn and spleen tyrosine kinase (SYK), and activates Bruton's tyrosine kinase (BTK), triggering the activation of multiple key signalling pathways and transcription factors that regulate B cell proliferation, differentiation and apoptosis in a cell maturation-dependent manner [4].

Membrane-recruited BTK undergoes auto-phosphorylation and then activates phospholipase C γ 2 (PLC γ 2) [5] which further catalyses the hydrolysis of phosphatidylinositol 4,5-bisphosphate (PIP $_2$) into diacylglycerol (DAG) and inositol trisphosphate (IP $_3$). Intracellular calcium levels increase as a result of IP $_3$ production, thus providing the cofactors required for classical protein kinase C (PKC: PKC α , β I/II and γ) isoform activation [6]. PKC isoforms, specifically PKC β II in B cells, activate survival pathways through NF- κ B-mediated signalling [7], thus linking proximal BCR-mediated signals with downstream pathways. CLL cells exhibit a dysregulated PKC isoform expression profile: upregulation of PKC β II, PKC ϵ , PKC ζ and downregulation of PKC α and PKC β I compared to normal B cells, with the increased levels of PKC β II expression correlating with the poor prognostic outcome for CLL patients [8]. Furthermore, ZAP-70 recruits PKC β II to lipid rafts in CLL cells, which activates and enhances the translocation of PKC β II to the mitochondria where it phosphorylates the anti-apoptotic protein BCL2 [9].

PKC β has been shown to play an essential role in the regulation of leukaemia development in the TCL1 mouse model of CLL, as indicated by the abrogation of leukemic cells in PKC β KO mice [10]. We developed a CLL-like mouse model, by introducing a kinase-inactive PKC α (PKC α -KR) construct in mouse hematopoietic stem/progenitor cells (HSPCs), which resulted in the development of an aggressive subset of CLL *in vitro* and *in vivo*, exhibiting an upregulation of ZAP-70, enhanced proliferation and increased tumour load in the lymphoid organs [11]. Analysis of the PKC isoform profile in PKC α -KR-transformed cells revealed that similar to that seen in primary CLL samples, PKC β II expression was upregulated, and this occurred at later stages of disease development [12]. Here, we determine the importance of PKC β expression in disease development in our mouse model, analyse the mechanisms that promote PKC β upregulation and delineate the signalling pathways that occur downstream of BTK/PKC β , which may have particular importance in developing future therapies for B cell malignancies.

2. Materials and Methods

2.1. Primary Cells and Cell Lines

HSPCs obtained from the foetal liver (FL) of wild-type ICR mice on day 14 of gestation were prepared as described previously, and retrovirally transduced with a plasmid encoding either empty vector control (MIEV) or MIEV-PKC α -KR (PKC α -KR) with the bicistronic expression of GFP. Maintenance of the retroviral constructs within the cells during the cultures was assessed by GFP expression using flow cytometry [11]. Immediately prior to analysis, MIEV and PKC α -KR cells were removed from OP9 monolayers and placed on empty 6 well plates for 2 h to remove carry-over OP9 cells. All cell lines were routinely tested for mycoplasma contamination. All mice were maintained at the University of Glasgow Central Research Facilities under standard animal housing conditions in accordance with local and home office regulations. Primary CLL cells, obtained from patients that had given informed consent, were isolated as described previously [13] and cryopreserved for future use. Clinical details of patients used in these studies are presented in Supplementary Table S1; none of the patients had received chemotherapy within the preceding 3 months.

2.2. Surface and Intracellular Staining and Flow Cytometric Analysis

Flow cytometry reagents used are detailed in Supplementary Table S2, including the mouse CLL surface markers (CD19-APC-Cy7, CD5-APC, CD23-PE-Cy7, CD45-PerCP) and

phospho-BTK antibodies (BTK^{Y223}-AF647, BTK^{Y551}-AF647). After drug treatment/stimulation as indicated, MIEV and PKC α -KR cells ($\geq 1 \times 10^6$ cell/condition) were stained as described previously [11]. Cells were acquired using a FACSCantoII flow cytometer with BD FACSDiva software and analysed using FlowJo (Tree Star Inc., Ashland, OR, USA) software.

2.3. Cell Stimulation/Drug Treatment

MIEV and PKC α -KR cells ($\geq 1 \times 10^6$ /condition) were treated with 1 μ M ibrutinib (IB) or 20 μ M enzastaurin (Enza) or vehicle control in 10% FBS/ α MEM media as previously published [12]. Primary CLL cells were pre-incubated with 1 μ M IB, 10 μ M Enza or vehicle control in 10% FBS/RPMI media on ice and then stimulated with 10 μ g/mL F(ab')₂ fragment anti-human IgM (Stratech Scientific Ltd., Ely, UK) to crosslink the BCR (BCR-XL) at 37 °C and then analysed.

2.4. Cell Counting Beads

To compare cell counts between different co-culture conditions, a set volume of Count-Bright beads (BD Biosciences, Wokingham, UK) was added to each PKC α -KR sample as indicated, prior to flow cytometry. After FSC/SSC gating on the beads, 2000 beads were acquired together with a variable cell number to enable a relative cell number to be calculated between samples [14].

2.5. Proliferation/Apoptosis Assays

MIEV and PKC α -KR cells ($\geq 1 \times 10^6$ /condition) were labelled with CellTrace Violet (CTV; 2 μ M) using CellTrace™ Cell Proliferation Kits (Life Technologies, Paisley, UK) as described previously [14]. Cells were analysed on the FACSCantoII flow cytometer. Results are expressed relative to the mean fluorescence intensity (MFI) of CTV in no drug control (NDC) cells at 48 h. At the end of the stimulations/drug treatment incubations, cells were stained with Annexin V/7-AAD as described previously [13].

2.6. Lentiviral Knockdown of *prkcb*

Lentiviral knockdown vectors targeting mouse *prkcb* and non-targeting control (SCR) were purchased from Sigma-Aldrich (St. Louis, MO, USA) in the pLKO.1 backbone. Lentiviral particles were generated using a three-plasmid HEK293T lentiviral protocol, as described previously [15]. Briefly, HEK293 cells were transfected overnight using CaCl₂ and 2 \times HBS containing pHIV1 and VSV-G as accessory plasmids. The virus was collected in DMEM supplemented with 20% FCS and freshly isolated HSPCs (d0) were cultured in a viral medium supplemented with 4 μ g/mL polybrene and IL7/Flt3 (10 ng/mL each). This was repeated 4 times over 48 h. After transduction, the cells were washed and re-suspended in complete media. Cell sorting for GFP⁺CD19⁺CD45⁺CD11b⁻ cells was performed using FACS Aria™ III cell sorter (BD Biosciences) on day 7; MIEV and PKC α -KR were then introduced by retroviral transduction on day 8 as described previously [11].

2.7. qPCR

RNA was extracted from MIEV- or PKC α -KR-transduced cells from day 17–23 co-cultures using RNeasy mini kit (Qiagen, Manchester, UK) according to the manufacturer's protocol. Synthesis of cDNA was performed using SuperScript® III Reverse transcriptase (Life Technologies) as per the manufacturer's protocol. Real-time PCR (qPCR) was conducted using the TaqMan PCR Master Mix (Applied Biosystems, Warrington, UK), with glyceraldehyde-3-phosphate dehydrogenase (*gapdh*) used as a reference control. Invented primers and probes and PCR buffers were purchased from Applied Biosystems unless otherwise stated. *Egr1* and *Btk* primers were designed and optimised, using TATA-box binding protein (*tbp*) as a reference control (Supplementary Table S3). For each PCR reaction, 1 μ L cDNA was used followed by an appropriate primer master mix containing 0.25 μ M forward, 0.25 μ M reverse primers and 2xSYBR Green PCR Mastermix (ThermoFisher Scientific, Paisley, UK). Technical triplicates of each PCR reaction were performed. qPCR

was performed on the 7900HT Fast Real-Time PCR System (Applied Biosystems): The cycle condition for 40 cycles is as follows: 95 °C 2 min, 40 cycles of 95 °C 5 s, 60 °C 10 s, 72 °C 5–20 s. All primer pairs were optimised to ensure efficient amplification of a single PCR product. NDC or MIEV was used as the calibrator and data were analysed using the $2^{-\Delta\Delta CT}$ relative quantification method.

2.8. Chromatin Immunoprecipitation (ChIP)

MIEV- and PKC α -KR-transduced cells were co-cultured on OP9 cells until days 20–23, as described above. The cells were harvested and IP was performed on the sonicated chromatin material using a ChIP grade antibody—anti-SP1 antibody (Clone D4C3; Cell Signaling Technologies, Danvers, MA, USA) or IgG (negative control), as described previously [16]. The primer sets were designed on regions flanking three SP1 binding regions within the *prkcb* promoter (Supplementary Table S4).

2.9. Microarrays

MIEV- or PKC α -KR-transduced HSPCs were co-cultured on OP9 cells in the presence of IL-7 for 17–23 days (late co-culture) and total RNA was isolated using an RNeasy kit (Qiagen, Manchester, UK) from five independent co-cultures. The RNA was quantified using a Nanodrop ND-1000 Spectrophotometer (ThermoFisher Scientific). Screening of the RNA samples was performed against Affymetrix™ GeneChip® Mouse Gene 1.0 ST Array (Santa Clara, CA, USA). Background correction and normalisation of generated CEL files were performed using Robust Multichip Average (RMA) in Partek Genomics Suite 7.19.1125 (St. Louis, MO, USA). Differentially expressed genes, PKC α -KR vs. MIEV, were detected by one-way analysis of variance. Significant genes ($n = 2836$), were identified with a fold change ± 1.2 and p -value < 0.05 , with 1513 up- and 1323 downregulated in PKC α -KR vs. MIEV.

2.10. Western Blots

Cell lysates were prepared in lysis buffer (1% Triton, 1 mM 1,4-dithiothreitol (DTT), 2 mM ethylenediaminetetraacetic acid (EDTA), 20 mM Tris pH 7.5 containing a complete protease inhibitor, and PhosStop; Roche) from early (day 6–12) or late (day 15–23) MIEV and PKC α -KR cells, or primary CLL cells, with or without drug treatment as indicated and quantified using the Bradford Assay (ThermoFisher Scientific). The antibodies used are described in Supplementary Table S5, and Western blotting was performed as described previously [14]. Images were developed using an SRX 101A film processor.

2.11. Migration Assay

MIEV- or PKC α -KR-transduced cells (2×10^5) were incubated in 100 μ L RPMI-1640/0.5% BSA media in the presence or absence of drugs (as indicated) for 30 min prior to the assay. Cells were then transferred to the upper chamber of a 6.5 mm diameter Transwell culture insert (Costar®, Fisher Scientific, Loughborough, UK.) and placed into wells containing 600 μ L media supplemented with 150 ng/mL CXCL12. The cells were incubated for 4 h at 37 °C. Thereafter, three 150 μ L aliquots were removed from each lower chamber for counting by flow cytometry. The total number of events acquired during 20 s on high flow setting was recorded for each aliquot.

2.12. Statistics

p values were determined by students paired or unpaired t -test or mixed model ANOVA on a minimum of at least 3 biological replicates to compare data using GraphPad Prism 6 software (GraphPad Software Inc., San Diego, CA, USA) as indicated; *, **, *** and **** represent $p < 0.05$, 0.01, 0.001 and < 0.0001 , respectively. Biological replicates were derived from individual cell culture conditions from distinct biological samples. Results are presented as mean \pm standard error of the mean of biological replicates (SEM), with the number of replicates performed highlighted in the figure legends.

3. Results

3.1. PKC β Promotes Leukemogenesis in the PKC α -KR CLL-like Mouse Model

We and others have previously demonstrated that PKC β II is upregulated in CLL mouse models (E μ -Tcl-1 and PKC α -KR; [12]) and in primary CLL samples, particularly in poor prognostic samples suggesting a role in CLL pathogenesis [8]. To extend this research we addressed the importance of *prkcb* expression during the initiation of the CLL-like disease in our PKC α -KR mouse model. Performing *prkcb* shRNA knockdown (KD) experiments prior to retroviral transduction with PKC α -KR revealed that the generation of the leukemic phenotype was negatively impacted upon the reduction in *prkcb* expression. There was a significant reduction in surface expression of the leukemic marker characteristic of this CLL model, CD23 and CD5 (Figure 1A,B, Supplementary Figure S1), as well as CD45 expression. An additional feature of PKC α -KR-transduced cells is an increased cellular count in the cultures, which was significantly reduced, together with elevated apoptosis in *prkcb* KD conditions (Figure 1C,D). A significant reduction in PKC β mRNA levels was confirmed in cultured cells transduced with sh-*prkcb*, compared with SCR controls (Figure 1E). The reduced cell numbers generated with PKC α -KR-transduced *prkcb* KD cells precluded us from testing whether CLL-like development was blocked in vivo. Taken together, these results indicate that PKC β plays an important role in the initiation of CLL in our mouse model, supporting previous findings in the E μ -Tcl-1 CLL mouse model [10].

3.2. Sp1 Regulates Similar Transcriptional Networks in the PKC α -KR CLL-like Cells and Primary Human CLL Samples

The transcription factor SP1 plays a central role in *PRKCB* gene regulation in human CLL [17]. We were interested in determining whether the *prkcb* gene was similarly regulated by Sp1 in our CLL mouse model. The *prkcb* promoter contains three Sp1 binding regions (Figure 2A). ChIP analysis revealed that Sp1 binding to the *prkcb* promoter was significantly upregulated in PKC α -KR transduced CLL-like cells at all three Sp1 binding sites, compared with MIEV cells (Figure 2B). These data were supported with experiments using mithramycin (mtm), an anti-cancer antibiotic that selectively binds G-C-rich DNA sequences to inhibit RNA and DNA polymerases and globally displace Sp1 [18]. Treatment of PKC α -KR cells with 200 nM mtm significantly reduced Sp1 binding activity at all regions assessed on the *prkcb* promoter (Figure 2C). We have previously shown that PKC β II is upregulated in PKC α -KR cells compared with MIEV cells [12], and mtm treatment resulted in a downregulation of PKC β II protein expression specifically in PKC α -KR cells, although this downregulation did not reach significance (Figure 2D, Supplementary Figure S2). Assessing the wider impact of mtm treatment on transcriptional changes in our PKC α -KR cells revealed a reduction in expression not only of *prkcb*, but also *Sp1* itself and *Bcl2*, *Vegfa*, *Blnk* and *Lef1* upon treatment with mtm, compared to no drug control (NDC; Figure 2E), a result similar to that seen in human CLL samples (Supplementary Table S6). Taken together, these data suggest a similar regulation of Sp1-mediated transcription networks between poor prognostic human CLL cells and PKC α -KR CLL cells.

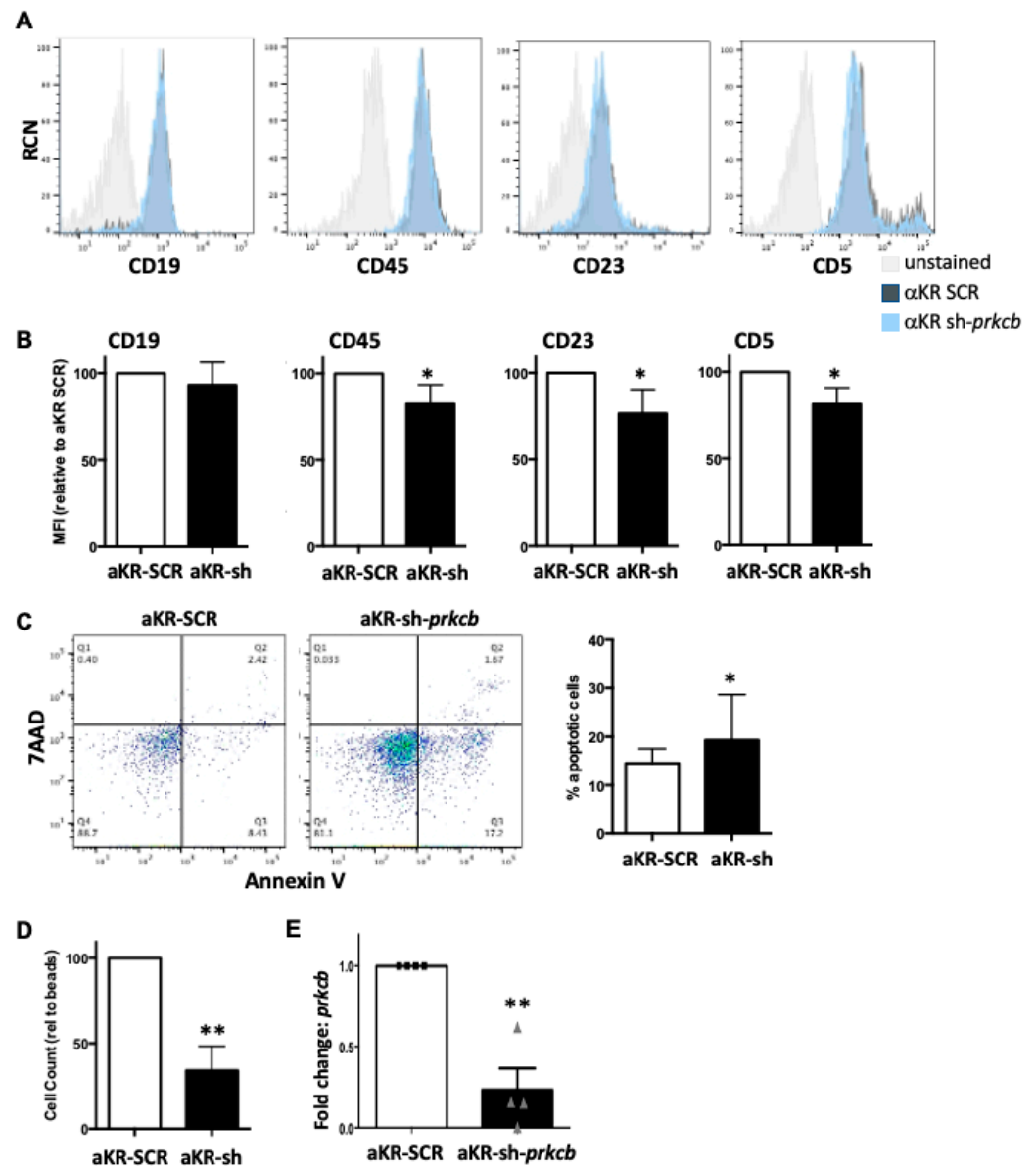


Figure 1. Reduction in PKC β expression inhibits the initiation of PKC α -KR-mediated CLL development. Knockdown of *prkcb* (or scrambled (SCR) control) was performed in HSPC cells within 24 h of isolation from the mouse, then these cells were retrovirally transduced with MIEV or PKC α -KR (α KR) at d7. Cells were co-cultured with OP9 in the presence of cytokines for up to 35 days. Phenotypic characterisation of the cells was carried out by flow cytometry analysing: (A) CD19, CD45, CD23 and CD5. Representative histogram plots are shown, gated on FSC/SSC and GFP+ cells comparing α KR sh-*prkcb* cells with α KR-SCR cells compared with unstained cells (gating strategy shown in Supplementary Figure S1); (B) Average MFIs of CD19, CD45, CD23 and CD5 surface markers are shown relative to α KR-SCR cultures ($n = 5$); (C) Apoptosis was determined by AnnV/7AAD staining. A representative dot plot shows Annexin V vs. 7AAD staining in α KR-SCR cells and α KR sh-*prkcb*. The graph shows the percentage apoptotic (AnnV+) cells present in cultures post d14 ($n = 5$); (D) Cell counts were performed with flow cytometry using counting beads, shown relative to a set bead number acquired ($n = 5$); (E) qPCR analysis of *prkcb* expression, α KR-SCR (circles) compared with α KR sh-*prkcb* (triangles). *Gapdh* was used as the reference gene and α KR-SCR-transduced cells were used as a calibrator ($n = 4$). All experiments shown are representative of $n \geq 4$ biological replicates as indicated. Paired student *t*-test with Wilcoxon matched-pair signed rank test was used to analyse the data. * $p < 0.05$, ** $p < 0.01$.

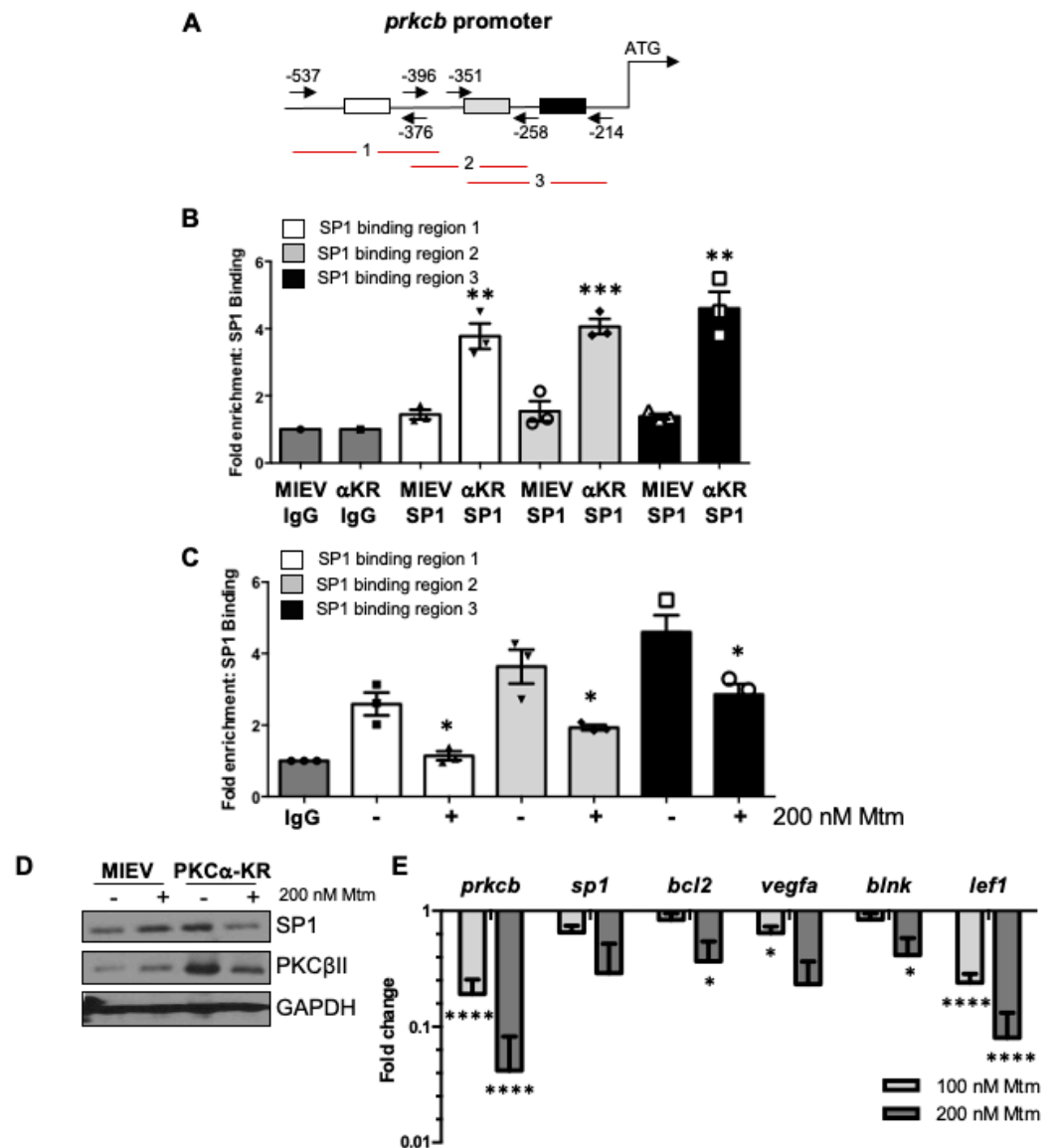


Figure 2. Sp1 binding is upregulated in the *prkcb* promoter of PKCα-KR transduced CLL-like cells. (A) Diagram showing Sp1 binding sites at the *prkcb* promoter, the primer locations and the three products; (B) ChIP analysis was performed in MIEV (binding region 1 (black triangles), 2 (white circles), 3 (white triangles)) and PKCα-KR cells (binding region 1 (inverted triangles), 2 (diamonds), 3 (squares)) at the late stage of co-culture (> d17) to determine Sp1 binding occupancy at the *prkcb* promoter (average of *n* = 3 biological replicates); (C) ChIP analysis was performed in PKCα-KR cells in the absence (binding region 1 (black squares), 2 (inverted triangles), 3 (white squares)) and presence of 200 nM mithramycin (mtm; binding region 1 (triangles), 2 (diamonds), 3 (circles)) for 12 h to determine Sp1 binding at the *prkcb* promoter (average of *n* = 3 biological replicates); (D) The expression levels of Sp1 and PKCβII were determined by Western blotting in MIEV and PKCα-KR cells treated with 200 nM mtm (representative blot shown of *n* = 3 experiments; densitometry of the blots and the full blots shown in Supplementary Figure S2). (E) qPCR analysis of *prkcb*, *sp1*, *bcl2*, *vegfa*, *blink*, *lef1* genes in PKCα-KR cells upon treatment with mtm (average of *n* = 2/3 biological replicates, an average of technical duplicates). *Gapdh* was used as the reference gene and normalised to NDC. Unpaired student *t*-tests (B,C) or one-way ANOVA (E) were used to analyse the data (where biological triplicates were performed). * *p* < 0.05, ** *p* < 0.01, *** *p* < 0.001, **** *p* < 0.0001.

3.3. BCR Signalling Components Are Dysregulated in PKC α -KR CLL-like Cells

To investigate global gene expression profiles in the PKC α -KR CLL mouse model within the timeline of PKC β II upregulation, microarrays were performed comparing MIEV- and PKC α -KR-transduced cells at the late stage of B cell transformation (post d17 of co-culture after retroviral transduction with MIEV- and PKC α -KR-constructs at d0 [12]). Analysis of the dataset revealed differentially regulated gene expression between the MIEV- and PKC α -KR-transduced cells, and enrichment of pathways that were significantly dysregulated, with immune system processes identified as the most enriched group of pathways (Figure 3, Supplementary Table S7, Supplementary Figure S3). This analysis indicated an upregulation of genes allied to B cell activation in PKC α -KR-transduced cells, and given the importance of BCR signalling in the pathology of CLL, we chose to validate this pathway in our CLL mouse model (Figure 4). Deregulation of the BCR signalling in PKC α -KR-transduced cells, summarised in Figure 4A, is highlighted by a number of features including CD45 and CD19 upregulation in the CLL-like PKC α -KR cells (indicated in pink; previously confirmed by flow cytometry [12]), together with an upregulation of signalling components proximal to BCR-mediated signalling (*Lyn*, *Btk*, *Blnk*) while *Syk*, *Pten* and *Pdk1* are downregulated (indicated in green) compared to MIEV control cells. The expression of some transcription factors was dysregulated, with PKC α -KR cells showing upregulation of *Bcl6*, *Egr1*, *Elk1*, *NFkB* and *Foxo1*, while *Creb* and *Tcf1* were downregulated compared to MIEV control cells in the microarray datasets. Upregulation of *Egr1* and *Btk* in the late PKC α -KR cultures was confirmed by qPCR (Figure 4B). In support of the data shown in Figure 2E, *Prkcb* and *Lef1* expression patterns aligned with the *Sp1* expression, with downregulation of these genes in early PKC α -KR cultures, and significant upregulation in the late PKC α -KR cultures, compared to the respective MIEV cells (Figure 4C).

Analysing the expression levels of BCR signalling components demonstrated that key hubs proximal and distal to the BCR were dysregulated in the CLL-like PKC α -KR cells compared to MIEV control cells both at the early and late stages of the CLL-like disease. *Lyn*, *Egr1* and c-Myc expressions were upregulated, while *Lck* was downregulated (Figure 5A,C, Supplementary Figures S4 and S5). PKC α expression was significantly downregulated in the PKC α -KR cells, in agreement with our previous work [12]. Furthermore, a significant elevation in pAKT^{S473} and pS6^{S235/236} was observed, indicating an elevation in AKT/mTOR-mediated signalling in PKC α -KR cultures (Figure 5A, Supplementary Figure S4). An upregulation in pc-Myc^{S62} was also observed, accompanied by an increase in c-Myc expression in PKC α -KR cells compared with MIEV suggesting a stabilisation of c-Myc in PKC α -KR cells; however, these modulations did not reach significance (Figure 5C, Supplementary Figure S5). Phospho-flow staining revealed a significant elevation of both BTK^{Y551} and BTK^{Y223} phosphorylation in PKC α -KR compared to MIEV cells (Figure 5B). Taken together these results indicate that PKC α -KR CLL-like cells exhibit upregulated BCR signalling activity.

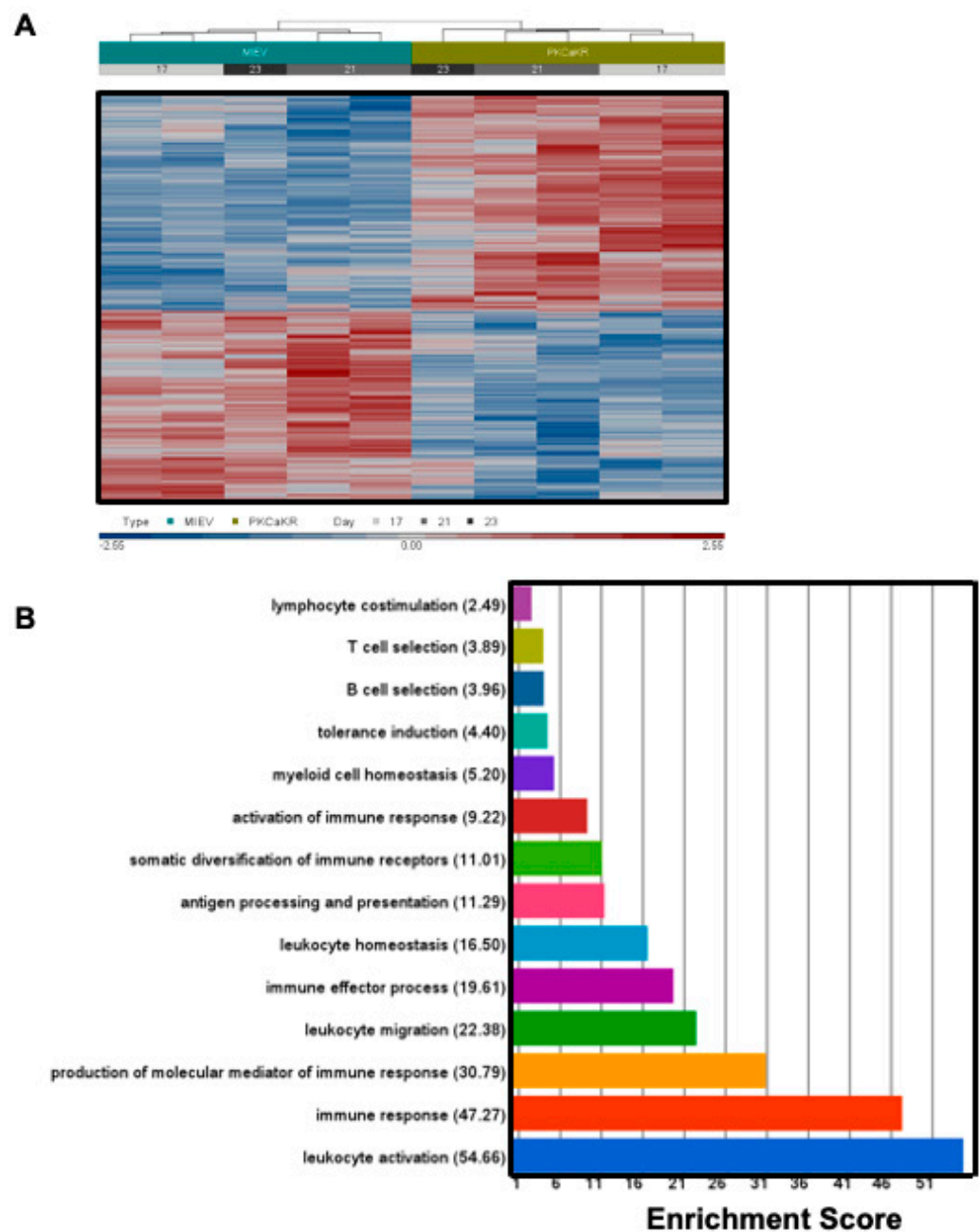


Figure 3. Gene expression comparisons between PKC α -KR vs. MIEV B lineage cells. **(A)** Hierarchical clustering of the relative gene expression using the Euclidian matrix with average linkage (Partek Genomics Suite, v6.6) for PKC α -KR vs. MIEV raw Affymetrix files ($n = 5$). Culture day for each column identified in grey for both PKC α -KR and MIEV cells (day 17, 21 or 23). **(B)** Gene ontology enrichment analysis of the significantly altered genes (fold change ± 1.2 and p -value < 0.05) between late co-culture PKC α -KR vs. MIEV cells, identified immune system processes as the most enriched groups of pathways. Functional groups with the highest over-representation of genes within the gene list compared to background are shown alongside their respective enrichment score ($-\log p$ -value of a chi-square test).

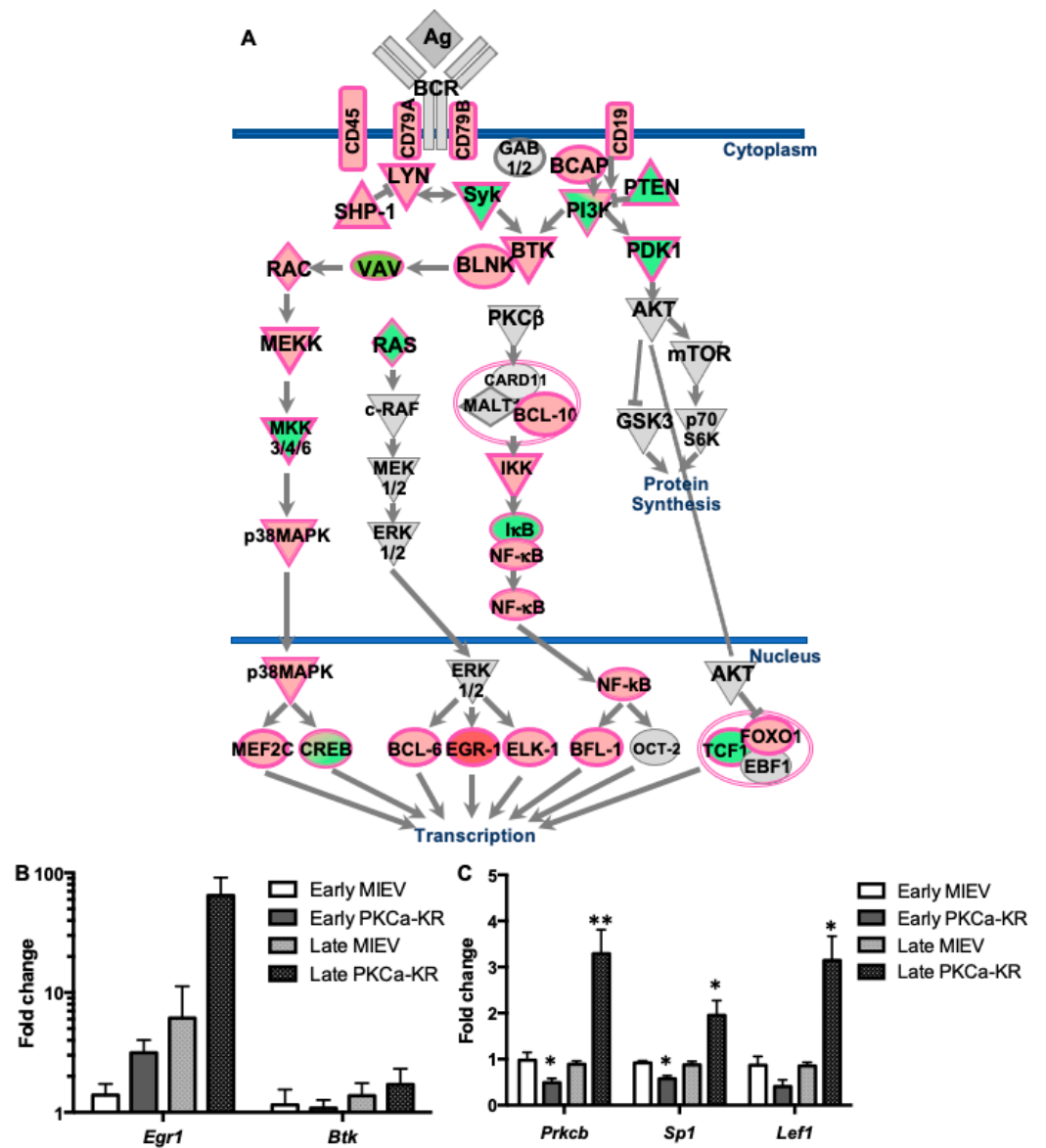


Figure 4. Global gene expression analysis revealed activation of the BCR-mediated signalling pathway in PKC α -KR cells. Global RNA analysis was performed using Affymetrix GeneChip mouse gene 1.0 ST on MIEV and PKC α -KR transduced cells at d17–23 in the B cell transformation co-culture. (A) Dysregulated components of the BCR pathway in PKC α -KR vs. MIEV cells isolated from late co-cultures ($n = 5$ PKC α -KR, $n = 5$ MIEV) were identified. Significantly up- and down-regulated components are highlighted in pink/red and green, respectively; (B) qPCR validation of *egr1* and *btk* genes, which were both upregulated in the microarray analysis at the late stage (d15–23) of B cell transformation, compared with the early stage (d6–10). Data are an average of $n = 2$ –4 biological replicates, normalised to *tbp*. (C) Comparison of *prkcb*, *sp1* and *lef1* gene expression in the early vs. late stages of B cell transformation co-cultures, determined by qPCR. Data represent $n = 3$ –5 biological replicates, normalised to *gapdh*. Unpaired student *t*-tests were used to analyse the data. * $p < 0.05$, ** $p < 0.01$.

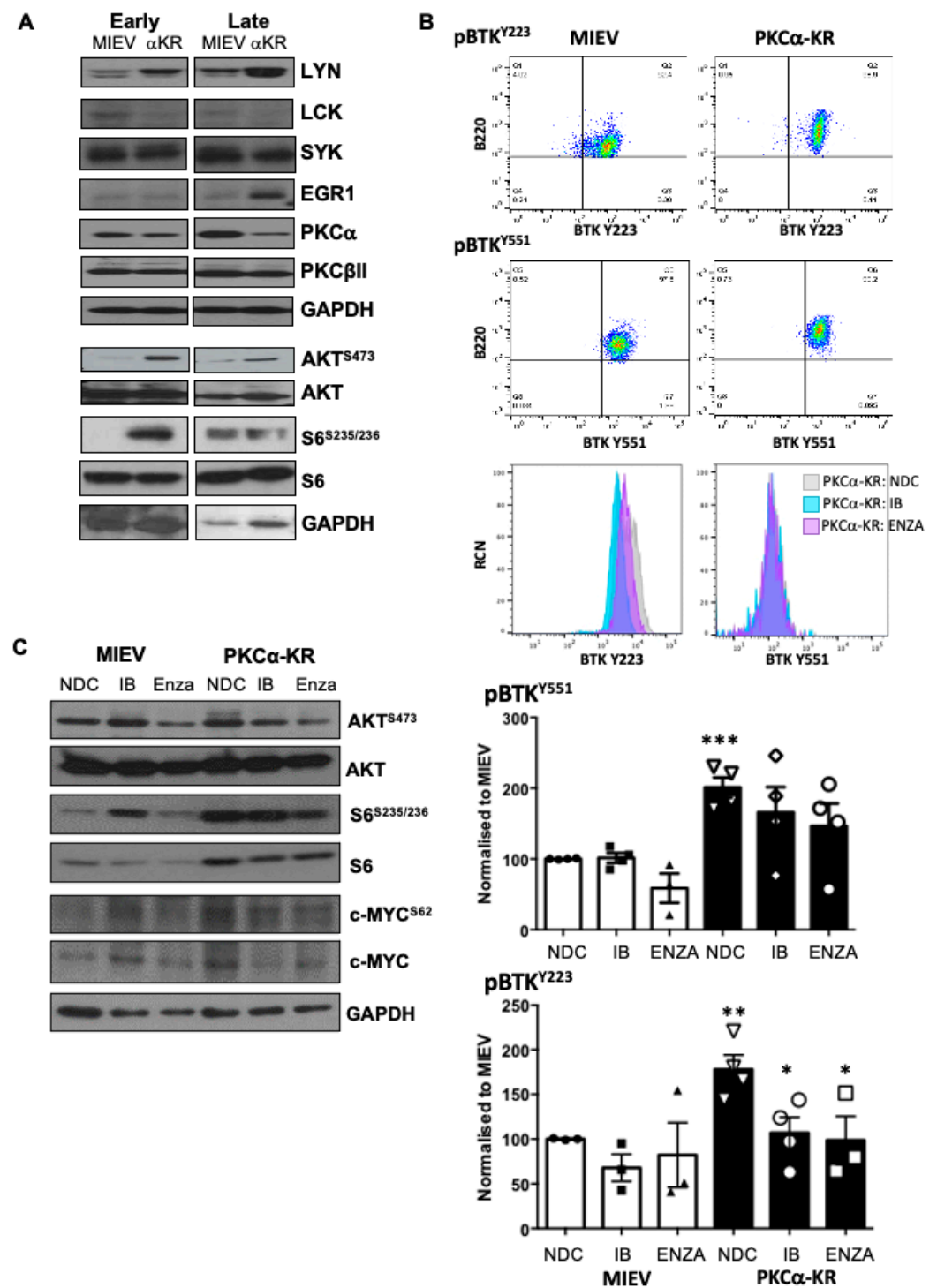


Figure 5. Inhibition of PKCβ activity downregulates key proteins in the BCR signalosome in mouse CLL model. (A) The expression/activation status of key hubs proximal and distal to the BCR pathway was analysed by Western blotting in early and late co-cultures of MIEV and PKCα-KR cells. Representative Western blots are shown. Densitometry of Western blots for these proteins ($n \geq 4$) is shown in Supplementary Figure S4. (B) Phospho-flow was used to analyse the levels of BTK^{Y551} and BTK^{Y223} phosphorylation in MIEV (left) and PKCα-KR (right) cells in the presence and absence of either Ibrutinib (IB; 1 μM) or enzastaurin (Enza; 20 μM). Upper panel shows the flow cytometry dot plots of the mouse B lineage cells (B220⁺) vs. phospho-BTK, gated on FSC/SSC, while lower histogram plots show the effect of drug treatments on BTK^{Y551} and BTK^{Y223} phosphorylation as overlay

(NDC—pale grey; IB—turquoise; ENZA—pink). Lower graphs show the average MFI of phospho-BTK normalised to MIEV no drug control (NDC; $n = 3/4$ independent experiments; MIEV—white bars (NDC (circles), IB (squares), ENZA (triangles), PKC α -KR—black bars (NDC (inverted triangles), IB (circles), ENZA (squares)). (C) MIEV and PKC α -KR cells were treated with either IB or Enza, or NDC. Representative Western blots are shown identifying the effect on key proteins within the BCR signalosome as indicated. Densitometry of the Western blots for these proteins ($n = 3$) is shown in Supplementary Figure S3. One-way ANOVA was used to analyse the data. * $p < 0.05$, ** $p < 0.01$, *** $p < 0.001$.

3.4. PKC α -KR CLL-like and Primary Human CLL Cells Share Similar Responses to BCR-Targeted Inhibitors

To determine how PKC β impacted BCR signalling, MIEV- and PKC α -KR-expressing cells were treated with either BTK inhibitor ibrutinib (IB) or PKC β II inhibitor enzastaurin (Enza). While the drug treatments did not affect the BTK phosphorylation on MIEV B-cells, IB- and Enza-treatment significantly reduced BTK^{Y223} phosphorylation suggesting an inhibition in BTK activity in the PKC α -KR-expressing B cells (Figure 5B). The elevation in S6^{S235/236} phosphorylation in PKC α -KR-expressing cells was inhibited by Enza treatment. The elevation in c-Myc^{S62} phosphorylation and c-Myc expression in PKC α -KR cells was not significantly affected by drug treatments (Figure 5C, Supplementary Figure S5). These findings suggest that PKC β plays a vital role in driving the activation of key proteins within the BCR-mediated BTK and AKT/mTOR signalling in PKC α -KR cells.

To establish whether our findings in the PKC α -KR CLL-like model were applicable to primary human CLL samples, we treated human CLL cells with IB or Enza in the presence of F(ab')₂ stimulation (BCR-XL) and assessed the phosphorylation/activation status of BTK. Both BTK^{Y551} and BTK^{Y223} phosphorylation levels were significantly downregulated upon PKC β inhibition with Enza in human CLL cells compared to NDC, while IB treatment led to a significant downregulation of BTK^{Y223} phosphorylation only (Figure 6A). Western blotting of primary CLL cell lysates stimulated with BCR-XL showed an elevation in phosphorylation of AKT^{S473} and pS6^{S3235/236} and an increase in c-Myc expression similar to that noted in PKC α -KR cells. Furthermore, a reduction in AKT^{S473} and pS6^{S3235/236} phosphorylation was more pronounced with Enza treatment in the presence of BCR-XL, although this did not reach significance. Enza significantly decreased overall c-Myc^{S62} phosphorylation upon BCR-XL; however, coupled with the significant reduction in total c-Myc protein with IB or Enza treatment, this led to a significant increase in pc-Myc^{S62} phosphorylation on the remaining c-Myc in human CLL cells (Figure 6B, Supplementary Figure S6), findings that mirrored trends in PKC α -KR CLL-like cells.

We have previously shown that Enza significantly and selectively impacts PKC α -KR cell viability (20 μ M) and proliferation (10 μ M) over MIEV cells [12]. Testing cell viability with increasing IB concentrations revealed that MIEV cells were more sensitive to IB than PKC α -KR cells up to a concentration of 10 μ M IB (Supplementary Figure S7). MIEV and PKC α -KR cells were similarly affected by IB treatment with a significant block in proliferation at 3 μ M (Figure 6C). As it has previously been established that inhibition of BCR-mediated signals with IB can reduce CLL cell migration towards CXCL12 [19], and leukocyte migration was the fourth most dysregulated pathway in PKC α -KR cells, the migration capacity of MIEV and PKC α -KR CLL-like cells was tested in the presence of IB or Enza treatment. Initial analysis of the adhesion marker CD38, which is regulated by BCR-mediated signalling, showed that surface expression of CD38 was upregulated on PKC α -KR cells compared with MIEV cells (Figure 6D) [20,21]. Our data revealed that PKC α -KR cells have a significantly enhanced migration ability towards SDF1 compared to MIEV cells (Figure 6E), likely due to elevated surface expression of CXCR4 and CD38 (Figure 6D, Supplementary Figure S8), and elevated BCR-mediated signalling. However, while migration was significantly inhibited upon treatment with either IB or Enza, these treatments did not alter the surface expression of CD38 (Supplementary Figure S9).

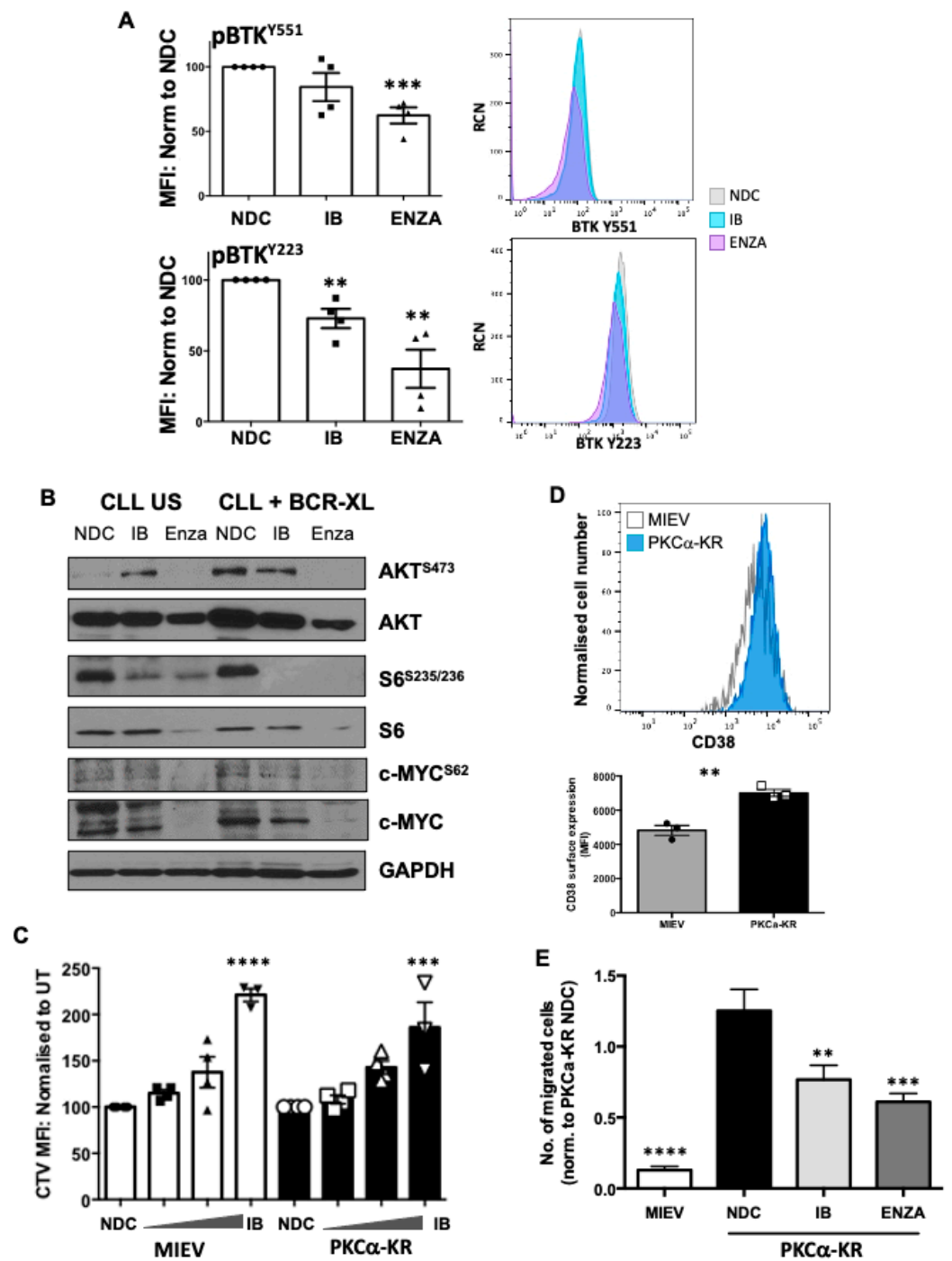


Figure 6. Inhibition of PKC β upon treatment with enzastaurin downregulates key proteins within the BCR signalosome in primary CLL cells. (A,B) Human CLL cells were treated with 1 μ M IB or 10 μ M Enza in the presence or absence of BCR crosslinking (BCR-XL; F(ab')₂ fragment stimulation). A. Phospho-flow was used to analyse the levels of BTK^{Y551} and BTK^{Y223} phosphorylation upon treatment with drugs \pm BCR-XL. Left-Graphs show the average MFI of the individual phospho-BTK sites as indicated, normalised to MIEV NDC ($n = 4$ individual patient samples; NDC (circles), IB (squares), ENZA (triangles)). Right-Histogram plots show the effect of drug treatments on BTK^{Y551} and BTK^{Y223} phosphorylation as overlay (NDC—pale grey; IB—turquoise; ENZA—pink); (B) Western blots were performed to identify the effect of drug treatment on key proteins within the BCR signalosome in human CLL cells. Representative Western blots are shown. Densitometry of the Western blots for these proteins ($n \geq 3$ individual patients) is shown in Supplementary Figure S6;

(C) Late co-culture MIEV and PKC α -KR cells (2×10^6) were labelled with CTV and cultured for 48 h in the presence (100 nM–3 μ M) of increasing concentrations of IB (squares, triangles, inverted triangles) or NDC (circles). Results are expressed as the CTV MFI relative to NDC cells for MIEV and PKC α -KR cultures ($n = 4$ individual experiments); (D) A histogram is shown comparing the surface expression of CD38 in MIEV and PKC α -KR cells taken from d33 of co-culture (upper) and the average MFI of CD38 expression is shown relative to MIEV cultures ($n = 3$); (E) Migration assessment of MIEV and PKC α -KR cells was performed in the presence and absence of 1 μ M IB or 20 μ M Enza. The data shown represent an average of 5 independent experiments. Unpaired student *t*-tests (D) or one-way ANOVA (A,C,E) were used to analyse the data. ** $p < 0.01$, *** $p < 0.001$, **** $p < 0.0001$.

4. Discussion

BCR signals are central to CLL pathogenesis, and PKC β is an important regulator of these signals in healthy and malignant B cells. Although we have known for many years that PKC β II is overexpressed in the malignant cells of CLL [8], the link between PKC β and leukemogenesis is not yet demonstrated. Here, we show that PKC β expression plays a central role in the development of leukemic cells in our model of CLL (PKC α -KR mouse model). Moreover, we show that the transcription factor SP1 is important for driving a transcription program that promotes leukemogenesis in our model system, and that this program is, at least in part, driven by PKC β activity. Importantly, this SP1-driven program is also observed in human CLL cells, suggesting a role for PKC β in the pathogenesis of the human disease.

The critical role played by PKC β in the development of normal B cells has long been established [22]: targeted disruption of the *prkcb* gene in mice results in a severe reduction in marginal zone and B1 populations, while our own work shows that overexpression of PKC β II expands these B cell populations [23]. In contrast, the PKC α knockout mouse model has no phenotype in early B lymphocyte development or proliferation and to date, this model has not been associated with the development of haematological malignancies [24]. Indeed, PKC α -deficient mice display an increased risk of developing colorectal cancer which similar to CLL, exhibits a reduction in PKC α expression and an elevation in PKC β II expression in patient samples [25]. In the current study, we demonstrate that both CD5 and CD23 were downregulated in PKC α -KR-transduced cells on a background of *prkcb* KD in vitro. This is distinct from the PKC β -deficient mice, which only exhibited a reduction in CD5⁺ B1 B cells, with surface CD23 expression on B cell populations being unaffected [22]. This indicates that *prkcb* KD targets the leukemic phenotype present in the PKC α -KR mouse model. A relationship between PKC β and CLL pathogenesis was suggested in studies showing overexpression of this isoform in the malignant cells of this disease, particularly in cells from patients with late-stage disease [8]. More recently, PKC β was found to play a critical role in disease development in the E μ -TCL1 CLL mouse model, with no leukaemia development in the absence of PKC β expression [10]. Subsequent studies of this model highlighted the essential role played by PKC β II within the stromal compartment in promoting both maintenance and chemosensitivity of malignant B cells [26,27] but did not address whether this PKC isoform was involved in the initiation of malignant cell transformation. Our work provides clarity to this question and shows that PKC β expression is important for leukemogenesis in our model of CLL, a model we have previously shown is similar to human CLL with respect to overexpression of PKC β II in the leukemic cells [12]. It is likely, however, that the role of PKC β in this context is one of facilitation rather than transformation because our earlier work has also shown malignant disease does not occur when this PKC isoform is specifically overexpressed in B cells [27]. A similar role for PKC β overexpression has been suggested for neoplastic transformation in colon cancer [25,28]. Another BCR pathway protein overexpressed in CLL cells, Lyn, is similar to PKC β in promoting the expansion of the malignant clone through its role within microenvironmental cells; however, it differs because Lyn deficiency does not affect the rate of malignant cell transformation in the E μ -Tcl1 murine model of CLL [29]. Thus, the current study

remains the first to directly implicate a signalling protein within the BCR pathway in CLL leukemogenesis.

Our data show that elevated PKC β expression in PKC α -KR-transduced cells is driven by elevated Sp1 binding activity at the *prkcb* promoter. This is similar to what is observed in human CLL cells [17] and suggests that the mechanisms controlling PKC β expression are accurately modelled by our system. A further similarity is demonstrated by our experiments using mtm to target the DNA binding activity of SP1. In addition to *prkcb* downregulation, mtm treatment reduces expression of *blnk*, *bcl2*, *vegfa*, *lef1* and *sp1* in the PKC α -KR-transduced cells, and mtm treatment of CLL cells results in comparable downregulation of the human orthologues of these genes. Sp1, a ubiquitous transcription factor, may play a significant role in promoting a gene transcription profile that induces CLL cell survival and is aligned with poor prognostic disease [30]. This notion is supported by recent work showing that targeted delivery of miR-29b to CLL cells leads to enhanced cellular reprogramming and decreased viability due to its effect of decreasing SP1 expression [31]. Furthermore, mtm analogues have been shown to be effective against CLL cells, with EC-7072 inducing CLL cell death through targeting of BCR signalling [32], and administration of MTM α 32E to the E μ -Tcl1 mouse model reduces the malignant cell burden [33].

BCR signalling strength in malignant cells of CLL correlates with poor disease prognosis. This has relevance to our model because it was one of the top dysregulated pathways in our microarray comparing gene expression between PKC α -KR-transduced and control cells. Biochemical analysis of the activation status of signalling pathways downstream of the BCR indicated that our mouse model possesses constitutively active BCR signalling, as shown by elevated phosphorylation of BTK^{Y223}, AKT^{S473}, S6^{S235/236} and c-Myc^{S62}, and increased expression of the early activation marker EGR1. We further noted a downregulation in Lck expression which has previously been described in BCR-activated CLL cells [34]. These findings validate our microarray data and consolidate our previous findings showing activation of the ERK-MAPK- and AKT/mTOR signalling pathways in PKC α -KR-expressing cells [11,12,35]. The significant upregulation of both BTK^{Y551} and BTK^{Y223} phosphorylation in our mouse model indicates that BTK is constitutively active, leading to activation of distal BCR-mediated signalling (i.e., ERK-MAPK pathway), and suggests that such phosphorylation may be aided by elevated Lyn kinase expression which is reported to target phosphorylation of BTK^{Y551} and promote downstream BCR signalling events [36]. A role for PKC β in regulating this phosphorylation event is shown in experiments using enzastaurin or ibrutinib. Both compounds inhibited BTK^{Y223} phosphorylation in PKC α -KR and primary CLL cells, causing a reduction in AKT/mTOR and ERK-MAPK/c-Myc mediated pathways. One difference between PKC α -KR and primary CLL cells in this respect is that enzastaurin also inhibited BTK^{Y551} phosphorylation in the latter but not the former. While this result may be related to the off-target effects of enzastaurin [37], it may suggest that PKC β II may have an impact on BCR signalling upstream of BTK activation. While the mechanism regulating PKC β II-mediated phosphorylation of BTK is not clear, it is interesting to note that PKC β II has been demonstrated to negatively regulate BTK by S180 phosphorylation to prevent its membrane recruitment [38]. Whether these two events are linked remains to be elucidated in future studies.

While it has been well established that ibrutinib has enhanced the survival of patients with B cell malignancies including CLL, mantle cell lymphoma and Waldenström's macroglobulinemia (WM) [39–41], clinical trials incorporating enzastaurin have not, as yet, revealed any significant improvement in patient survival in DLBCL [42]. Pre-clinical studies using sotrastaurin, a more broad-range PKC isoform inhibitor targeting α , β and θ isoforms, in CLL and DLBCL indicate a strong anti-tumour effect [43,44]. While the reasons for the lack of effect of enzastaurin are not entirely clear, it may be due to the study design as it was used as relapse prevention rather than as disease-active therapy in high-risk patients. Given the interest in developing appropriate models to test potential therapeutic compounds, we consider that our CLL-like mouse model provides an excellent model

for carrying out pre-clinical testing of novel BCR-targeted agents, that may be translated towards the clinic.

5. Conclusions

The data reported here demonstrate a role for PKC β in the development of leukemic B cells in our model and suggest it may be important for facilitating leukemogenesis in CLL. This has implications for the current understanding of CLL pathogenesis where signalling through the BCR pathway is important. Although many of the kinases in this pathway are overexpressed in CLL cells, PKC β is the only one currently that facilitates the neoplastic transformation of these cells. Moreover, the current study validates our PKC α -KR model for the study of CLL cells, where many responses observed using PKC α -KR CLL cells are similar to that of primary CLL cells. Given this parallel, we consider that this CLL-like mouse model will be an excellent tool to decipher the pathobiological behaviour of CLL cells.

Supplementary Materials: The following supporting information can be downloaded at: <https://www.mdpi.com/article/10.3390/cancers14236006/s1>. Figure S1: Gating strategy for cell surface marker expression, Figure S2: Mithramycin treatment of PKC α -KR cells leads to a slight decrease in PKC β II expression, Figure S3: Gene ontology enrichment analysis, Figure S4: PKC α -KR cells modulate BCR signaling components in a similar manner to primary CLL cells, Figure S5: Drug treatments modulate BCR signaling components in CLL-like PKC α -KR cells, Figure S6: Drug treatments modulate signaling components in BCR-crosslinked primary CLL samples, Figure S7: The effect of ibrutinib treatment on the viability of PKC α -KR-CLL-like cells, Figure S8: Expression of CXCR4 on the surface of hematopoietic co-cultures, Figure S9: The surface expression of adhesion marker CD38 was unaffected by drug treatments, Table S1: CLL patient clinical characteristics, Table S2: Flow Cytometry Antibodies, Table S3: PCR primer sequences, Table S4: ChIP primer sequences for the Sp1 binding sites on the mouse *prkcb* promoter region, Table S5: List of antibodies used for Western blotting, Table S6 Gene modulation in primary CLL cells upon treatment with mithramycin, Table S7 Gene ontology analysis of the significantly altered genes between late co-culture PKC α -KR vs. MIEV cells identifies the most enriched group of pathways.

Author Contributions: J.H. and A.T. contributed equally to this manuscript. Conceptualisation, N.K., J.R.S. and A.M.M.; Data curation, J.H., A.T., A.K.H. and A.M.M.; Formal analysis, J.H., A.T., H.A.M., B.H.L. and A.M.M.; Funding acquisition, A.A., J.R.S. and A.M.M.; Investigation, J.H., A.T., A.K.H., K.M.D., J.C., N.M., A.F.K., I.S., J.L. and H.N.B.A.; Methodology, J.H., A.T. and A.M.M.; Supervision, N.K., J.R.S. and A.M.M.; Writing—original draft, J.H., A.T., J.R.S. and A.M.M.; Writing—review and editing, J.H., A.T., A.K.H., H.A.M., K.M.D., A.A., B.H.L., J.C., N.M., A.F.K., I.S., J.L., H.N.B.A., N.K., J.R.S. and A.M.M. All authors have read and agreed to the published version of the manuscript.

Funding: This research was funded by a project grant from LLR (Blood Cancer UK—Ref. 13012). Cell sorting facilities were funded by the Kay Kendall Leukaemia Fund (KKL501) and the Howat Foundation. AT was funded by a Bloodwise project grant (13012), AH was supported by a KKL Clinical training fellowship (KKL838), JH was funded by a Bloodwise (BCUK) project grant (18003), NM was funded by an MRC-DTP PhD studentship (MR/K501335/1).

Institutional Review Board Statement: The studies for use of primary CLL patient samples were approved by the West of Scotland Research Ethics Service, NHS Greater Glasgow and Clyde (UK) and all work was carried out in accordance with the approved guidelines (REC Ref: 20/WS/0066). The animal study protocol was approved by the local University of Glasgow Animal Welfare and Ethical Review Board and the UK Home Office (PPL: PD6C67A47 approved in January 2018).

Informed Consent Statement: Informed consent was obtained from all subjects involved in the study.

Data Availability Statement: Microarray data presented in Figure 3 are available at the Gene Expression Omnibus (GEO) repository (GSE185075). The microarray data presented in Supplementary Table S6 are available at the GEO repository (GSE210348).

Acknowledgments: The authors thank the CLL patients for donating blood samples for this study.

Conflicts of Interest: The authors declare no conflict of interest.

References

1. Stevenson, F.K.; Forconi, F.; Packham, G. The meaning and relevance of B-cell receptor structure and function in chronic lymphocytic leukemia. *Semin. Hematol.* **2014**, *51*, 158–167. [[CrossRef](#)] [[PubMed](#)]
2. Hamblin, T.J.; Davis, Z.; Gardiner, A.; Oscier, D.G.; Stevenson, F.K. Unmutated Ig V(H) genes are associated with a more aggressive form of chronic lymphocytic leukemia. *Blood* **1999**, *94*, 1848–1854. [[CrossRef](#)] [[PubMed](#)]
3. Burger, J.A.; Chiorazzi, N. B cell receptor signaling in chronic lymphocytic leukemia. *Trends Immunol.* **2013**, *34*, 592–601. [[CrossRef](#)] [[PubMed](#)]
4. Slupsky, J.R. Does B cell receptor signaling in chronic lymphocytic leukemia cells differ from that in other B cell types. *Scientifica* **2014**, *2014*, 208928. [[CrossRef](#)]
5. Park, H.; Wahl, M.I.; Afar, D.E.; Turck, C.W.; Rawlings, D.J.; Tam, C.; Scharenberg, A.M.; Kinet, J.P.; Witte, O.N. Regulation of Btk function by a major autophosphorylation site within the SH3 domain. *Immunity* **1996**, *4*, 515–525. [[CrossRef](#)]
6. Michie, A.M.; Nakagawa, R. Elucidating the role of protein kinase C in chronic lymphocytic leukaemia. *Hematol. Oncol.* **2006**, *24*, 134–138. [[CrossRef](#)]
7. Shinohara, H.; Yasuda, T.; Aiba, Y.; Sanjo, H.; Hamadate, M.; Watarai, H.; Sakurai, H.; Kurosaki, T. PKC β regulates BCR-mediated IKK activation by facilitating the interaction between TAK1 and CARMA1. *J. Exp. Med.* **2005**, *202*, 1423–1431. [[CrossRef](#)]
8. Abrams, S.T.; Lakum, T.; Lin, K.; Jones, G.M.; Treweeke, A.T.; Farahani, M.; Hughes, M.; Zuzel, M.; Slupsky, J.R. B-cell receptor signaling in chronic lymphocytic leukemia cells is regulated by overexpressed active protein kinase C β II. *Blood* **2007**, *109*, 1193–1201. [[CrossRef](#)]
9. zum Büschenfelde, C.M.; Wagner, M.; Lutzny, G.; Oelsner, M.; Feuerstacke, Y.; Decker, T.; Bogner, C.; Peschel, C.; Ringshausen, I. Recruitment of PKC- β II to lipid rafts mediates apoptosis-resistance in chronic lymphocytic leukemia expressing ZAP-70. *Leukemia* **2010**, *24*, 141–152. [[CrossRef](#)]
10. Holler, C.; Piñón, J.D.; Denk, U.; Heyder, C.; Hofbauer, S.; Greil, R.; Egle, A. PKC β is essential for the development of chronic lymphocytic leukemia in the TCL1 transgenic mouse model: Validation of PKC β as a therapeutic target in chronic lymphocytic leukemia. *Blood* **2009**, *113*, 2791–2794. [[CrossRef](#)]
11. Nakagawa, R.; Soh, J.W.; Michie, A.M. Subversion of PKC α signaling in hematopoietic progenitor cells results in the generation of a B-CLL-like population in vivo. *Cancer Res.* **2006**, *66*, 527–534. [[CrossRef](#)] [[PubMed](#)]
12. Nakagawa, R.; Vukovic, M.; Tarafdar, A.; Cosimo, E.; Dunn, K.; McCaig, A.M.; Holroyd, A.; McClanahan, F.; Ramsay, A.G.; Gribben, J.G.; et al. Generation of a poor prognostic chronic lymphocytic leukemia-like disease model: PKC α subversion induces an upregulation of PKC β II expression in B lymphocytes. *Haematologica* **2015**, *100*, 499–510. [[CrossRef](#)] [[PubMed](#)]
13. McCaig, A.M.; Cosimo, E.; Leach, M.T.; Michie, A.M. Dasatinib inhibits B cell receptor signalling in chronic lymphocytic leukaemia but novel combination approaches are required to overcome additional pro-survival microenvironmental signals. *Br. J. Haematol.* **2011**, *153*, 199–211. [[CrossRef](#)] [[PubMed](#)]
14. Cosimo, E.; McCaig, A.M.; Carter-Brzezinski, L.J.; Wheadon, H.; Leach, M.T.; Le Ster, K.; Berthou, C.; Durieu, E.; Oumata, N.; Galons, H.; et al. Inhibition of NF- κ B-mediated signaling by the cyclin-dependent kinase inhibitor CR8 overcomes prosurvival stimuli to induce apoptosis in chronic lymphocytic leukemia cells. *Clin. Cancer Res.* **2013**, *19*, 2393–2405. [[CrossRef](#)] [[PubMed](#)]
15. Harris, W.J.; Huang, X.; Lynch, J.T.; Spencer, G.J.; Hitchin, J.R.; Li, Y.; Ciceri, F.; Blaser, J.G.; Greystoke, B.F.; Jordan, A.M.; et al. The histone demethylase KDM1A sustains the oncogenic potential of MLL-AF9 leukemia stem cells. *Cancer Cell.* **2012**, *17*, 473–487. [[CrossRef](#)]
16. Tarafdar, A.; Dobbin, E.; Corrigan, P.; Freeburn, R.; Wheadon, H. Canonical Wnt signaling promotes early hematopoietic progenitor formation and erythroid specification during embryonic stem cell differentiation. *PLoS ONE* **2013**, *8*, e81030. [[CrossRef](#)]
17. Al-Sanabra, O.; Duckworth, A.D.; Glenn, M.A.; Brown, B.R.; Angelillo, P.; Lee, K.; Herbert, J.; Falciani, F.; Kalakonda, N.; Slupsky, J.R. Transcriptional mechanism of vascular endothelial growth factor-induced expression of protein kinase C β II in chronic lymphocytic leukaemia cells. *Sci. Rep.* **2017**, *7*, 43228. [[CrossRef](#)]
18. Ray, R.; Snyder, R.C.; Thomas, S.; Koller, C.A.; Miller, D.M. Mithramycin blocks protein binding and function of the SV40 early promoter. *J. Clin. Investig.* **1989**, *83*, 2003–2007. [[CrossRef](#)]
19. de Rooij, M.F.M.; Kuil, A.; Geest, C.R.; Eldering, E.; Chang, B.Y.; Buggy, J.J.; Pals, S.T.; Spaargaren, M. The clinically active BTK inhibitor PCI-32765 targets B-cell receptor- and chemokine-controlled adhesion and migration in chronic lymphocytic leukemia. *Blood* **2012**, *119*, 2590–2594. [[CrossRef](#)]
20. Zupo, S.; Isnardi, L.; Megna, M.; Massara, R.; Malavasi, F.; Dono, M.; Cosulich, E.; Ferrarini, M. CD38 expression distinguishes two groups of B-cell chronic lymphocytic leukemias with difference responses to anti-IgM antibodies and propensity to apoptosis. *Blood* **1996**, *88*, 1365. [[CrossRef](#)]
21. Lanham, S.; Hamblin, T.; Oscier, D.; Ibbotson, R.; Stevenson, F.; Packham, G. Differential signaling via surface IgM is associated with VH gene mutational status and CD38 expression in chronic lymphocytic leukemia. *Blood* **2003**, *101*, 1087. [[CrossRef](#)] [[PubMed](#)]
22. Leitges, M.; Schmedt, C.; Guinamard, R.; Davoust, J.; Schaal, S.; Stabel, S.; Tarakhovskiy, A. Immunodeficiency in protein kinase c β -deficient mice. *Science* **1996**, *273*, 788–791. [[CrossRef](#)] [[PubMed](#)]
23. Azar, A.A.; Michie, A.M.; Tarafdar, A.; Malik, N.; Menon, G.K.; Till, K.J.; Vlatkovic, N.; Slipsky, J.R. A novel transgenic mouse strain expressing PKC β II demonstrates expansion of B1 and marginal zone B cell populations. *Sci. Rep.* **2020**, *10*, 13156. [[CrossRef](#)]

24. Pfeifhofer, C.; Gruber, T.; Letschka, T.; Thuille, N.; Lutz-Nicoladoni, C.; Hermann-Kleiter, N.; Braun, U.; Leitges, M.; Baier, G. Defective Ig2a/2b class switching in PKC alpha-/- mice. *J. Immunol.* **2006**, *176*, 6004. [[CrossRef](#)]
25. Gökmen-Polar, Y.; Murray, N.R.; Velasco, M.A.; Gatalica, Z.; Fields, A.P. Elevated protein kinase C betaII is an early promotive event in colon carcinogenesis. *Cancer Res.* **2001**, *61*, 1375–1381. [[PubMed](#)]
26. Lutzny, G.; Kocher, T.; Schmidt-Supprian, M.; Rudelius, M.; Klein-Hitpass, L.; Finch, A.J.; Duris, J.; Wagner, M.; Haferlach, C.; Seifert, M.; et al. Protein kinase c- β -dependent activation of NF- κ B in stromal cells is indispensable for the survival of chronic lymphocytic leukemia B cells in vivo. *Cancer Cell.* **2013**, *23*, 77–92. [[CrossRef](#)]
27. Park, E.; Chen, J.; Moore, A.; Mangolini, M.; Santoro, A.; Boyd, J.R.; Schjerven, H.; Ecker, V.; Buchner, M.; Williamson, J.C.; et al. Stromal cell protein kinase C- β inhibition enhances chemosensitivity in B cell malignancies and overcomes drug resistance. *Sci. Transl. Med.* **2020**, *12*, eaax9340. [[CrossRef](#)]
28. Murray, N.R.; Davidson, L.A.; Chapkin, R.S.; Clay Gustafson, W.; Schattenberg, D.G.; Fields, A.P. Overexpression of protein kinase C betaII induces colonic hyperproliferation and increased sensitivity to colon carcinogenesis. *J. Cell Biol.* **1999**, *145*, 699–711. [[CrossRef](#)]
29. Nguyen, P.H.; Fedorchenko, O.; Rosen, N.; Koch, M.; Barthel, R.; Winarski, T.; Florin, A.; Wunderlich, F.T.; Reinary, N.; Hallek, M. LYN kinase in the tumor microenvironment is essential for the progression of chronic lymphocytic leukemia. *Cancer Cell.* **2016**, *30*, 610–622. [[CrossRef](#)]
30. Wu, W.; Zhu, H.; Fu, Y.; Shen, W.; Miao, K.; Hong, M.; Xiu, W.; Fan, L.; Young, K.H.; Liu, P.; et al. High LEF1 expression predicts adverse prognosis in chronic lymphocytic leukemia and may be targeted by ethacrynic acid. *Oncotarget* **2016**, *7*, 21631–21643. [[CrossRef](#)]
31. Chiang, C.L.; Goswami, S.; Frizzera, F.W.; Xie, Z.; Yan, P.S.; Bundschuh, R.; Walker, L.A.; Huang, X.; Mani, R.; Mo, X.M.; et al. ROR1-targeted delivery of miR-29b induces cell cycle arrest and therapeutic benefit in vivo in a CLL mouse model. *Blood* **2019**, *134*, 432–444. [[CrossRef](#)]
32. Lorenzo-Herrero, S.; Sordo-Bahamonde, C.; Bretones, G.; Payer, Á.R.; González-Rodríguez, A.P.; González-García, E.; Perez-Escuredo, M.; Villa-Alvarez, J.; Nunez, L.E.; Moris, F.; et al. The Mithralog EC-7072 Induces Chronic Lymphocytic Leukemia Cell Death by Targeting Tonic B-Cell Receptor Signaling. *Front. Immunol.* **2019**, *10*, 2455. [[CrossRef](#)] [[PubMed](#)]
33. Rivas, J.R.; Liu, Y.; Alhakeem, S.S.; Eckenrode, J.M.; Marti, F.; Collard, J.P.; Zhang, Y.; Shaaban, K.A.; Muthusamy, N.; Hilderbrandt, G.C.; et al. Interleukin-10 suppression enhances T-cell antitumor immunity and responses to checkpoint blockade in chronic lymphocytic leukemia. *Leukemia*, **2021**; *online ahead of print*.
34. Schleiss, C.; Carapito, R.; Fornecker, L.M.; Muller, L.; Paul, N.; Tahar, O.; Pichot, A.; Taviani, M.; Nicolae, A.; Miguet, L.; et al. Temporal multiomic modeling reveals a B-cell receptor proliferative program in chronic lymphocytic leukemia. *Leukemia* **2021**, *35*, 1463–1474. [[CrossRef](#)]
35. Cosimo, E.; Tarafdar, A.; Moles, M.W.; Holroyd, A.K.; Malik, N.; Catherwood, M.A.; Hay, J.; Dunn, K.M.; Macdonald, A.M.; Guichard, S.M.; et al. AKT/mTORC2 inhibition activates FOXO1 function in CLL cells reducing B cell receptor-mediated survival. *Clin. Cancer Res.* **2019**, *25*, 1574–1587. [[CrossRef](#)]
36. Wahl, M.I.; Fluckiger, A.C.; Kato, R.M.; Park, H.; Witte, O.N.; Rawlings, D.J. Phosphorylation of two regulatory tyrosine residues in the activation of Bruton's tyrosine kinase via alternative receptors. *Proc. Natl. Acad. Sci. USA* **1997**, *94*, 11526–11533. [[CrossRef](#)] [[PubMed](#)]
37. Graff, J.R.; McNulty, A.M.; Hanna, K.R.; Konicek, B.W.; Lynch, R.L.; Bailey, S.N.; Banks, C.; Capen, A.; Goode, R.; Lewis, J.E.; et al. The protein kinase Cbeta-selective inhibitor Enzastaurin (LY317615.HCl), suppresses signalling through the AKT pathway, induces apoptosis, and suppresses growth of human colon cancer and glioblastoma xenografts. *Cancer Res.* **2005**, *65*, 7462–7469. [[CrossRef](#)]
38. Kang, S.W.; Wahl, M.I.; Chu, J.; Kitaura, J.; Kawakami, Y.; Kato, R.M.; Tabuchi, R.; Tarakhovskiy, A.; Kawakami, T.; Turck, C.W.; et al. PKCbeta modulates antigen receptor signaling via regulation of Btk membrane localization. *EMBO J.* **2001**, *20*, 5692–5702. [[CrossRef](#)] [[PubMed](#)]
39. Coutre, S.E.; Furman, R.R.; Flinn, I.W.; Burger, J.A.; Blum, K.; Sharman, J.; Jones, J.; Wierda, W.; Zhao, W.; Heerema, N.A.; et al. Extended Treatment with Single-Agent Ibrutinib at the 420 mg Dose Leads to Durable Responses in Chronic Lymphocytic Leukemia/Small Lymphocytic Lymphoma. *Clin. Cancer Res.* **2017**, *23*, 1149–1155. [[CrossRef](#)]
40. Treon, S.P.; Tripsas, C.K.; Meid, K.; Warren, D.; Varma, G.; Green, R.; Argyropoulos, K.V.; Yang, G.; Cao, Y.; Xu, L.; et al. Ibrutinib in previously treated Waldenstrom's macroglobulinemia. *N. Engl. J. Med.* **2015**, *372*, 1430–1440. [[CrossRef](#)]
41. Wang, M.L.; Rule, S.; Martin, P.; Goy, A.; Auer, R.; Kahl, B.S.; Jurczak, W.; Advani, R.H.; Romaguera, J.E.; Williams, M.E.; et al. Targeting BTK with ibrutinib in relapsed or refractory mantle-cell lymphoma. *N. Engl. J. Med.* **2013**, *369*, 507–516. [[CrossRef](#)]
42. Crump, M.; Leppä, S.; Fayad, L.; Lee, J.J.; Rocco, A.D.; Ogura, M.; Hagberg, H.; Schnell, F.; Rifkin, R.; Mackensen, A.; et al. Randomized, Double-Blind, Phase III Trial of Enzastaurin Versus Placebo in Patients Achieving Remission After First-Line Therapy for High-Risk Diffuse Large B-Cell Lymphoma. *J. Clin. Oncol.* **2016**, *34*, 2484–2492. [[CrossRef](#)] [[PubMed](#)]
43. El-Gamal, D.; Williams, K.; LaFollette, T.D.; Cannon, M.; Blachly, J.S.; Zhong, Y.; Woyach, J.A.; Williams, E.; Awan, F.T.; Jones, J.; et al. PKC- β as a therapeutic target in CLL: PKC inhibitor AEB071 demonstrates preclinical activity in CLL. *Blood* **2014**, *124*, 1481–1491. [[CrossRef](#)] [[PubMed](#)]
44. Naylor, T.L.; Tang, H.; Ratsch, B.A.; Enns, A.; Loo, A.; Chen, L.; Lenz, P.; Waters, N.J.; Schuler, W.; Donken, B.; et al. Protein kinase C inhibitor sotrastaurin selectively inhibits the growth of CD79 mutant diffuse large B-cell lymphomas. *Cancer Res.* **2011**, *71*, 2643–2653. [[CrossRef](#)] [[PubMed](#)]